Expression and purification of single cysteine-containing mutant variants of the mouse prion protein by oxidative refolding

Ishita Sengupta, Jayant B. Udgaonkar[*]

National Centre for Biological Sciences, Tata Institute of Fundamental Research, Bengaluru 560065, India

A B S T R A C T

The folding and aggregation of proteins has been studied extensively, using multiple probes. To facilitate such experiments, introduction of spectroscopically-active moieties in to the protein of interest is often necessary. This is commonly achieved by specifically labelling cysteine residues in the protein, which are either present naturally or introduced artificially by site-directed mutagenesis. In the case of the recombinant prion protein, which is normally expressed in inclusion bodies, the presence of the native disulfide bond complicates the correct refolding of single cysteine-containing mutant variants of the protein. To overcome this major bottleneck, a simple purification strategy for single tryptophan, single cysteine-containing mutant variants of the mouse prion protein is presented, with yields comparable to that of the wild type protein. The protein(s) obtained by this method are correctly folded, with a single reduced cysteine, and the native disulfide bond between residues C178 and C213 intact. The β-sheet rich oligomers formed from these mutant variant protein(s) are identical to the wild type protein oligomer. The current strategy facilitates sample preparation for a number of high resolution spectroscopic measurements for the prion protein, which specifically require thiol labelling.

© 2017 Elsevier Inc. All rights reserved.

1. Introduction

The site-specific incorporation of spectroscopically-active probes into proteins has facilitated a suite of high resolution *in vitro* experiments, spanning a range of length scales [1—3], allowing unprecedented structural characterization of protein structure and dynamics. Many of these probes are introduced into the protein of interest *via* thiol labelling, which additionally demands the purification and characterization of cysteine-containing mutant variants of the wild type (WT) protein. While this is relatively straightforward to do for proteins which lack native disulfide bonds, it can get complicated for proteins which do. The introduction of additional cysteine residues can lead to scrambling and incorrect disulfide bond pairing during expression and purification, resulting in misfolding, aggregation and/or precipitation [4—6].

The problem is further aggravated for proteins which are expressed in inclusion bodies [7,8], where inefficient refolding to their correctly folded native state hinders protein production in quantities typically required for *in vitro* experiments. The development of efficient protocols for the successful refolding of proteins with native disulfide bonds expressed in inclusion bodies in sufficient yields is therefore of great interest [5,9].

The prion protein is an example of such a protein with a native disulfide bond, that is normally expressed in inclusion bodies, and has been refolded and purified in several different ways [10—12]. Purification of the prion protein in a soluble form, though uncommon, has also been reported [13—15]. The prion protein is rich in α-helical content in its native monomeric form, but upon misfolding (under diseased conditions) forms β-sheet rich aggregates [16]. The misfolding and aggregation of the prion protein is responsible for a class of fatal neurodegenerative diseases, together known as spongiform encephalopathies. In contrast to the WT protein, the refolding of cysteine mutant variants of the prion protein has been challenging [17—21]. In the cases where these proteins have been purified, the yields were either too low, or rigorous characterization was not carried out.

The *in vitro* folding [22—25] and aggregation [26—29] of the WT as well as several pathogenic mutant variants of the prion protein [30—32] have been studied extensively. However, experiments which require labelling with spectroscopically-active probes, like paramagnetic nuclear magnetic resonance (NMR), electron paramagnetic resonance (EPR), fluorescence resonance energy transfer (FRET), fluorescence correlation spectroscopy (FCS) and thiol

---

labelling studies have remained largely unexplored for the prion protein [21,28].

The most common method for the purification of the WT protein employs affinity purification followed by reverse phase chromatography (RPC) [10,11]. When cysteine-containing mutant variants of the mouse prion protein (moPrP) were purified using this protocol, the protein was found to contain multimeric species, with a CD spectrum suggesting significant β-sheet content, unlike the WT protein. Refolding the protein to the native state while it was bound to the affinity column was also tried, but the yields from these preparations were too low for proper characterization and further experiments. It was therefore important to devise a protocol for the proper refolding of the cysteine-containing mutant variants of the prion protein, with sufficient yields and detailed characterization.

Here, a straightforward protocol for the expression and purification of single tryptophan, single cysteine-containing (single Trp, single Cys-containing) mutant variants of the full length moPrP with an intact native disulfide bond, is described. It is demonstrated, using two representative single Trp, single Cys-containing mutant variants of moPrP, W197−C223 and W144−C153 (mouse numbering has been used throughout this manuscript), that this method yields correctly folded highly pure protein in ample quantities, comparable to what has been reported for WT moPrP (Fig. 1). Moreover, the purification protocol has been shown to be applicable for a tryptophan-less (Trp-less) mutant variant which possesses the native disulfide bond, but lacks any additional cysteine residues.

The high refolding yields of single cysteine mutant variants of moPrP will enable many high resolution spectroscopic measurements to be carried out with ease, without the need for complicated and expensive protein production protocols.

2. Materials and methods

2.1. Reagents

All chemicals used for protein purification were purchased from HiMedia and Fisher Scientific, unless otherwise specified. Restriction Enzymes, DNA ligase, Phusion® High-Fidelity DNA Polymerase,

Fig. 1. Design of single Trp, single Cys-containing mutant variants of moPrP. The positions of tryptophans W197 and W144 and cysteines C153 and C223 are shown as blue sticks and red spheres, respectively, mapped on to the structure of the CTD of moPrP (PDB ID 1AG2) [33]. The secondary structural elements and the N- and C-termini are indicated. The disulfide bond between helix 2 and 3 is shown as a cyan stick. (For interpretation of the references to colour in this figure legend, the reader is referred to the web version of this article.)

dNTPs and DpnI enzyme from New England Biolabs and the DNA miniprep kit from Qiagen were used for molecular biology work. All reagents used for experiments were of the highest purity grade from Sigma Aldrich.
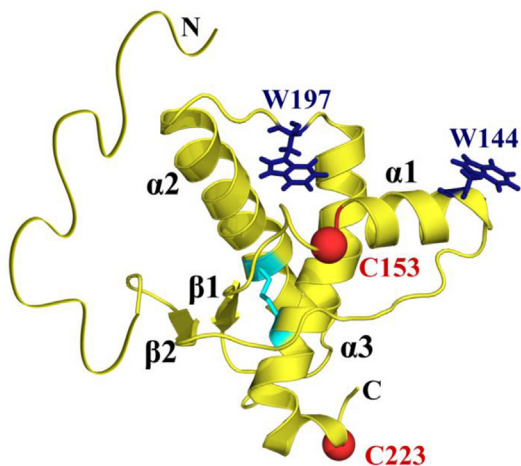
2.2. Plasmid construction

The backbone DNA of WT moPrP with all tryptophan residues mutated to phenylalanines was synthesized by GeneScript (USA) in a pUC57 vector. This was subcloned into the pET 22b(+) vector between the BamHI and NdeI restriction sites, for expression in E. coli. All mutations were made on this backbone, using standard site-directed mutagenesis protocols. First, mutations that would introduce single tryptophan residues were made on the Trp-less background, followed by mutations that would introduce single cysteine residues on these single Trp constructs. The cysteines C178 and C213 already present in the protein, which form the native disulphide bond were left unchanged. All constructs were verified by DNA sequencing before protein expression and purification.

2.3. Protein expression and purification

The pET-22b(+) plasmid encoding the single Trp, single Cys-containing mutant variant, or the Trp-less mutant variant of moPrP, were transformed into E. coli BL21(DE3) codon plus (Stratagene) cells. A single colony was used to inoculate 200 ml of LB media containing 100 μg/ml ampicillin, and grown at 37 °C for 8 h. A 50-mL portion of this primary culture was used to inoculate 500 ml of rich media, and grown for 3−3.5 h until it reached an OD_{600} of 1.8−2, when protein expression was induced using IPTG at a final concentration of 0.4 mM. The cells were allowed to grow for 12 h before harvesting and purification. The expressed protein was found to be present in inclusion bodies as described previously [11].

The pellet from 2 L of rich media (~40 g wet cell weight) was resuspended in 100 ml 20 mM Tris, pH 7.8 (Buffer A), and sonicated on ice with a Sonics Vibra-Cell™ Ultrasonic Liquid Processor for a total time of 20 min (5 s "on", 2 s "off") at a power level of 60%. This was centrifuged at 14,000 rpm and 4 °C for 30 min, and the supernatant discarded. The pellet was resuspended in 80 ml of Buffer A, sonicated for another 10 min (using the same settings), and centrifuged at 14,000 rpm and 4 °C for 30 min. The supernatant was discarded, and the pellet containing the inclusion bodies was solubilized in 80 ml of 6 M guanidinium hydrochloride (GdnHCl), 20 mM Tris, 1 mM reduced glutathione (GSH), pH 7.8 (Buffer G), and sonicated for a final 10 min. The pellet was disrupted manually with a glass rod, in between rounds of sonication to aid in solubilisation of the inclusion bodies. This was then centrifuged at 14,000 rpm and 4 °C for 45 min, and the supernatant containing the denatured protein was collected.

The supernatant was added to 30 ml of Ni Sepharose 6 Fast Flow beads (GE Healthcare), charged with nickel sulphate and equilibrated with Buffer G, and mixed by shaking on a rocker at room temperature (RT) for an hour with intermittent manual mixing. The equilibrated mixture was loaded in to a Vensil® glass column, and washed with 800 ml of Buffer G. The protein was finally eluted in 50 ml Buffer E (Buffer G + 200 mM imidazole, pH 7.8). The eluate was first dialyzed against 2 L of Buffer A containing 3 M GdnHCl and 1 mM GSH for 12 h followed by another round of dialysis against 2 L of Buffer A containing 1 M GdnHCl and 1 mM GSH for 12 h at 4 °C. Finally, to allow for correct disulfide formation, 0.06 g of oxidized glutathione (GSSG) was added to the protein solution (typically ~50 ml) to a final concentration of 0.2 mM, and stirred overnight at 4 °C. The protein was then dialyzed against 5 L of Buffer A (3 changes) to completely remove GdnHCl, GSH and GSSG. Some precipitation was seen at this stage, possibly due to misfolding and

aggregation, due to incorrect disulfide bond formation. The precipitate was removed by centrifugation at 20,000 rpm for 30 min, and the supernatant loaded on to a 5 ml HiTrap CM Sepharose FF column (GE Healthcare) that had been charged with Buffer A containing 2 M NaCl, using a peristaltic pump. The column was then attached to a GE ÄKTA purifier High Performance Liquid Chromatography System (HPLC), washed with 10 column volumes of washing buffer (Buffer A), followed by a gradient of 0—1 M NaCl in Buffer A, to elute the purified protein. The protein started eluting out at 35—40% of the gradient, corresponding to 350—400 mM NaCl (Fig. 2). The protein was then dialysed extensively against MQ water at 4 °C to remove all traces of NaCl, divided into aliquots, flash frozen and stored at −80 °C. All fractions were tested for the presence of protein on a 15% SDS-PAGE gel (Fig. 3). All chromatography steps were carried out at RT.

2.4. ESI-MS analysis

The identity of each protein was confirmed by electrospray ionization mass spectrometry (ESI-MS). The mass spectra showed
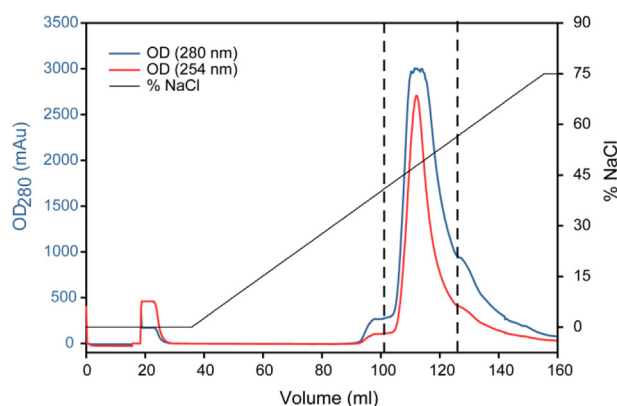
Fig. 2. Purification of single Trp, single Cys-containing moPrP (W197—C223) by cation-exchange chromatography. The protein started eluting at 35—40% NaCl (corresponding to 350—400 mM NaCl) in 20 mM Tris, pH 7.8, and fractions in between the vertical dashed lines were collected for dialysis and storage.
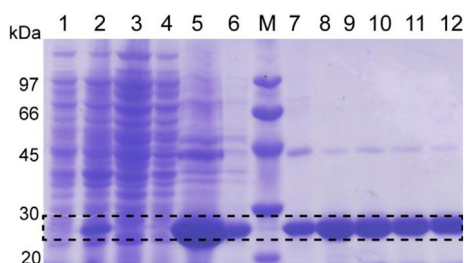
Fig. 3. Purification of single Trp, single Cys-containing moPrP (W197—C223) from inclusion bodies. Lane 1: Whole cell pellet before induction. Lane 2: Whole cell pellet 12 h after induction with 0.4 mM IPTG. Lanes 3 and 4: Soluble fractions after sonication rounds 1 and 2 respectively. Lane 5: Inclusion body fraction containing protein of interest. Lane 6: Wash from the Ni-NTA column. Lane M: Low MW SDS-PAGE marker. Lane 7: Eluate of the Ni-NTA column containing protein of interest. Lanes 8—12: Fractions eluting between ~35% and ~70% of NaCl from the CM-FF column (see Fig. 2). Note: Samples in lanes 5, 6 and 7 were initially present in GdnHCl. These samples were concentrated and washed multiple times with 8 M urea in a 10 kDa cut-off Centricon®, to remove all traces of GdnHCl before running on the gel. The intensity of the bands across all lanes is not representative of the total amount of protein in each fraction, as the same amount of protein could not be loaded in each well. The dashed line is a guide to the eye, to locate the position of W197—C223 moPrP on the gel. The expected mass of the protein is ~23 kDa.

that the single Trp, single Cys-containing mutant variants of moPrP each had a single glutathione moiety covalently attached to the additional cysteine (expected mass + 305 Da), and had the native disulfide bond intact. The Trp-less moPrP purified using the same protocol did not have the 305-Da adduct, unlike the single Trp, single Cys-containing mutant variants, due to the lack of an additional cysteine residue (Fig. 4).

2.5. Cleavage of the glutathione moiety by TCEP

Each protein aliquot was thawed on ice, and reduced with a 10-fold excess of tris(2-carboxyethyl)phosphine (TCEP) in 10 mM sodium acetate, pH 4.0 at 4 °C for 12 h, in the case of a solvent-exposed cysteine-containing variant, and for ~36 h for a buried cysteine-containing variant. This resulted in complete cleavage of the glutathione moiety. The protein solution was then desalted by passing through a Hi-Trap desalting column (GE Healthcare), to remove both the TCEP and the cleaved glutathione moiety, yielding the unlabelled protein, or processed further for labelling with spectroscopic probes. The unlabelled protein was flash frozen and stored at −80 °C, until further use. The identities of the unlabelled proteins were confirmed by mass spectrometry. Unlabelled protein concentration was measured using a calculated molar extinction coefficient of 22,450 $M^{-1}cm^{-1}$ at 280 nm (http://protcalc. sourceforge.net/) for the single Trp, single Cys-containing variants. For Trp-less moPrP, a calculated molar extinction co-efficient of 16,760 $M^{-1}cm^{-1}$ at 280 nm was used. The theoretical molar extinction co-efficients of single Trp, single Cys-containing mutant variants of moPrP, and of Trp-less moPrP were confirmed using a BCA assay (data not shown).
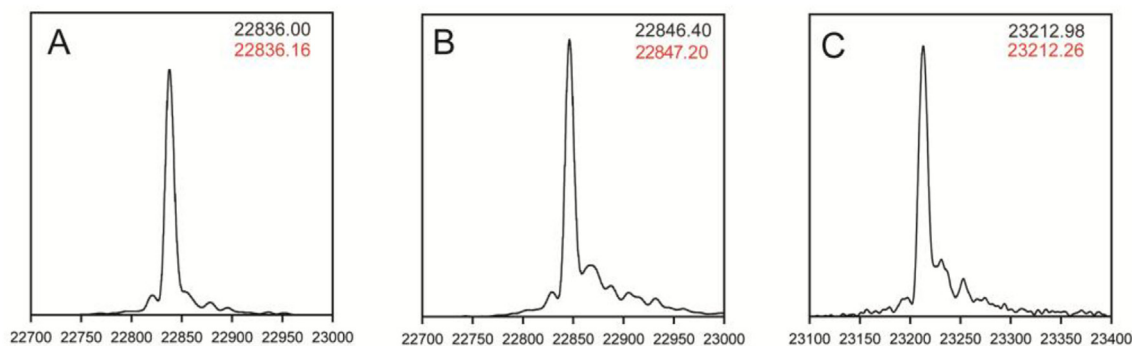
2.6. Spectrophotometric characterization of mutant protein variants

The purified single Trp, single Cys-containing mutant variants of moPrP were characterized spectrophotometrically by absorption, fluorescence, DLS and CD spectroscopy, and compared with WT moPrP.

The absorbance spectra were recorded on a CARY 300 double-beam spectrophotometer using a 10-mm path length cuvette. The fluorescence emission spectra were recorded from 310 to 450 nm on a Spex Fluoromax-4 spectrofluorimeter, with an excitation wavelength of 295 nm, excitation bandwidth of 1 nm and emission bandwidth of 5 nm. The far-UV CD spectra were acquired on a Jasco J-815 spectropolarimeter using a 0.1- cm path length cuvette, at a scan speed of 50 nm/min, response time of 2 s, and bandwidth of 1 nm. A final protein concentration of 10 μM in 10 mM sodium acetate buffer, pH 4 was used for these measurements. DLS measurements were carried out on monomer and oligomer samples, as described previously [11].

2.7. Oligomerization of the mutant protein variants at pH 4

Oligomerization was initiated by adding the appropriate volume of 10x aggregation buffer (100 mM sodium acetate, 1.5 M NaCl, pH 4) to protein, initially present in 10 mM sodium acetate, pH 4, mixed well and incubated at 37 °C. The final buffer composition was 10 mM sodium acetate, 150 mM NaCl, pH 4 and the final protein concentration was 100 μM. After incubation for 50 h, oligomerization was complete (estimated from the measurement of oligomerization kinetics, data not shown). The oligomers were diluted with 1x aggregation buffer such that the final protein concentration was 10 μM for spectrophotometric characterization.

Fig. 4. Mass spectrometric characterization of the mutant moPrP variants. ESI-MS spectra of (A) Trp-less, (B) W144−C153 (after TCEP reduction) and (C) W197−C223-GSH (before TCEP reduction) moPrP. The expected masses of the proteins are shown in red in each panel. (For interpretation of the references to colour in this figure legend, the reader is referred to the web version of this article.)

3. Results and discussion

3.1. Expression and purification of the single Trp, single Cys-containing mutant variants of moPrP

WT moPrP has an intrinsically disordered NTR (N-terminal region) and a globular CTD (C-terminal domain). The globular CTD consists of three α-helices and an antiparallel β-sheet (Fig. 1). A disulfide bond between residues C178 and C213 holds α2 and α3 together, and is crucial for the correct folding of the protein [33]. Disruption of the disulfide bond has been shown to cause misfolding and aggregation of the protein [34,35]. It is therefore essential that the correct disulfide bond be formed during the refolding and purification of monomeric prion protein.

WT moPrP is normally expressed in inclusion bodies and is refolded back to its native form during purification. The introduction of an additional cysteine into moPrP containing the native disulfide bond caused it to misfold, aggregate and precipitate during purification using the standardized protocol for purification of WT moPrP [11,36] and was thus deemed unsuitable. On-column refolding of the single cysteine-containing mutant variants was also attempted [28,37] but yielded very little protein, which was insufficient for experiments. It should be noted here that other purification protocols have been employed in the past to purify single and double cysteine-containing mutant variants of the prion protein, but yields were either not reported or too little in those studies [18,20,21,38]. It was therefore necessary to design a purification protocol which would facilitate the formation of the correct disulfide bond, without substantial loss of protein. Each mutant variant, like WT moPrP was found to be expressed in inclusion bodies (lane 5 in Fig. 3). Solubilized inclusion bodies (in buffer containing 6 M GdnHCl and 1 mM GSH) were purified using an affinity chromatography step. The protein was eluted under denaturing conditions (lanes 6 and 7 in Fig. 3). The unfolded protein was then allowed to refold by removing denaturant gradually by dialysis, in the presence of GSH. The addition of GSH ensured that all cysteines in the protein remained in the reduced form during refolding. Next, to allow for correct disulfide formation by the thiol-disulfide exchange reaction, the protein in 1 M GdnHCl was mixed with a small amount of GSSG, and left to react for 12 h. The formation of the correct disulfide bond is crucial for the prion protein, as in its absence, the native conformation is not attained. Finally, all denaturant and redox agents were removed by dialysis for the correctly folded, native monomeric state to be attained. The precipitation seen at this stage could be the result of non-native disulfide containing protein, which failed to fold to its native state on removal of denaturant. Interestingly, quick dilution of denaturant to promote folding had very poor refolding yields, even in the presence of the redox agent.

The single Trp, single Cys-containing mutant variant(s), purified in this manner always displayed a mass corresponding to a protein with a single glutathione adduct (expected + 305 Da). The expected mass was 2 Da less than the calculated mass, due to the formation of a single disulfide bond (Fig. 4b). This indicated that only a single cysteine was labelled with glutathione during purification, and that the other two cysteines were disulfide-bonded. Not surprisingly, the Trp-less moPrP, which had only the native disulfide-bonded cysteines and no additional cysteines, displayed the expected mass (Fig. 4a).

3.2. Preparation of unlabelled proteins for spectroscopic measurements

To cleave the glutathione moiety bound covalently to the additional cysteine in the protein without affecting the native disulfide bond, reduction with TCEP under native conditions was employed. The amount of TCEP and time of reduction were optimized depending on the extent of burial of the additional cysteine. Typically, for an exposed cysteine, 12 h of reduction at 4 °C was sufficient to completely cleave off the glutathione moiety, without reducing the native disulfide bond. The native disulfide bond is buried in the hydrophobic core of the protein, and remains protected against hydrogen exchange for more than 30 d [39] under native conditions. To remove TCEP and the cleaved glutathione moiety from the unlabelled protein, the protein was dialyzed against MQ water. The purity of the unlabelled proteins and extent of GSH cleavage was verified by mass spectrometry (Fig. 4b).

3.3. Spectrophotometric characterization of the mutant protein variants

The far-UV CD spectra of all mutant protein variants as well as the Trp-less moPrP were acquired and compared with that of WT moPrP. The overall secondary structure of the proteins was similar to the WT, confirming that the mutations did not perturb the secondary structure significantly (Fig. 5a). Moreover, it is known that when the naturally occurring disulfide-bonded cysteines in the prion protein is either reduced or mutated to other residues, the monomeric protein loses substantial α-helical structure [21,35]. The preservation of the overall fold of the proteins therefore provided further confirmation that the correct disulfide had indeed been formed. The absence of large aggregates from the protein preparation is evident from the absorbance spectra, which shows near-zero absorbance at and above 320 nm (Fig. 5b). Furthermore, DLS measurements confirmed that the protein(s) were indeed monomeric with a hydrodynamic radius (R_h) of ~2 nm (Fig. 5c).
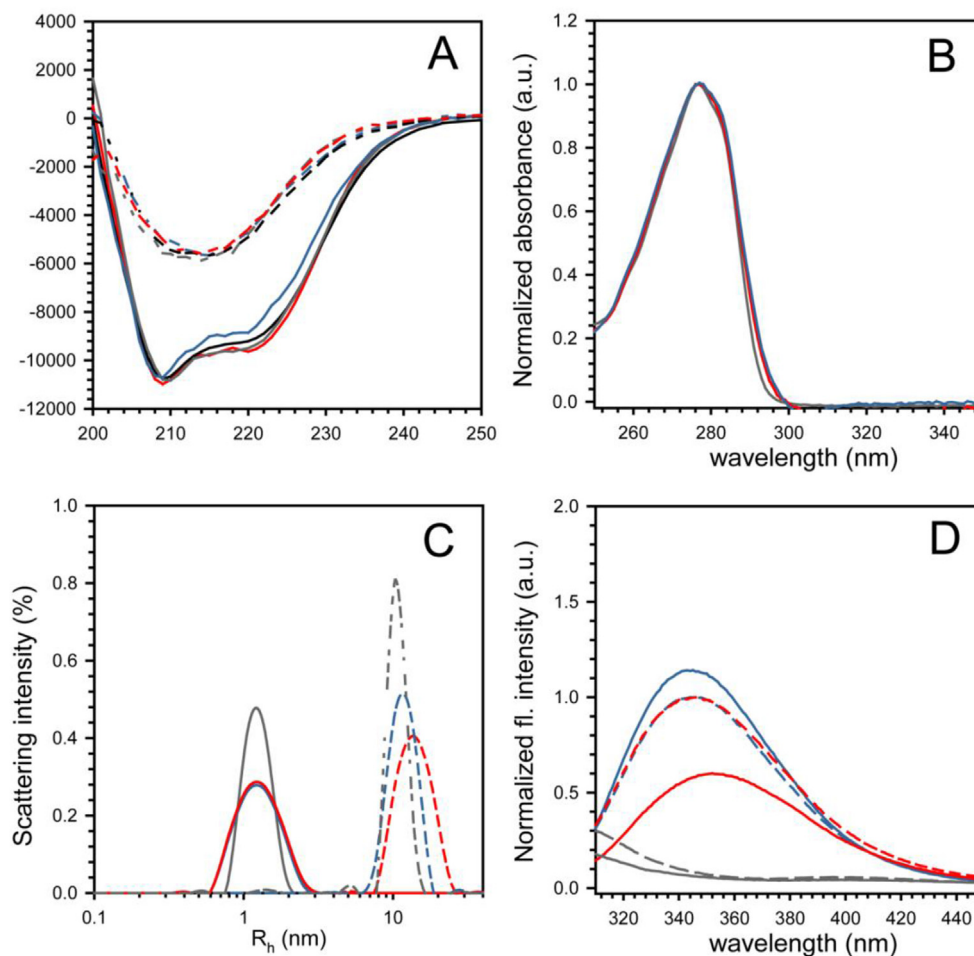
Fig. 5. Spectrophotometric characterization of the mutant moPrP variants. (A) Far-UV CD spectra of monomeric and oligomeric proteins. The solid blue, red, black and grey lines represent the far UV CD spectra of monomeric unlabelled W197−C223, W144−C153, WT and Trp-less moPrP, respectively. The corresponding dashed lines represent the far-UV CD spectra of the oligomeric proteins. (B) Absorbance spectra of monomeric proteins. The solid blue, red and grey lines represent the absorbance spectra of unlabelled W197−C223, W144−C153 and Trp-less moPrP, respectively. (C) DLS spectra of monomeric and oligomeric proteins. The solid blue, red and grey lines represent the DLS spectra of unlabelled W197−C223, W144−C153 and Trp-less moPrP, respectively. The corresponding dashed lines represent the DLS spectra of the oligomeric proteins (D) Fluorescence emission spectra of monomeric and oligomeric proteins. The solid blue, red and grey lines represent the fluorescence spectra of monomeric unlabelled W197−C223, W144−C153 and Trp-less moPrP, respectively. The corresponding dashed lines represent the fluorescence emission spectra of the oligomeric proteins. (For interpretation of the references to colour in this figure legend, the reader is referred to the web version of this article.)

Fluorescence spectra of monomeric and unlabelled W144−C153 and W197−C223 moPrP had emission maxima at 355 and 345 nm, respectively. This indicated that in the monomeric proteins, W144 was solvent-exposed, whereas W197 was partially buried from solvent [24,40]. These observations were in accordance with what was expected from the solution NMR structure (Fig. 1) [33].

3.4. Thermodynamic stability of mutant protein variants

From the urea-induced equilibrium unfolding curves, the thermodynamic stabilities of the unlabelled and Trp-less moPrP variants were determined [41] (Fig. 6). As can be seen from Table 1, the stabilities of all the mutant protein variants were similar to that of the WT moPrP. The mutations introduced in this study therefore did not drastically perturb the proteins, either in overall structure or stability. The mutant variants are good candidates for further experiments.

3.5. Oligomer formation by mutant protein variants

Trp-less, W144−C153 and W197−C223 moPrP were oligomerized for 50 h. At the end of 50 h, all mutant protein variants

were found to have oligomerized into a β-sheet rich conformation, which was confirmed by CD spectroscopy (Fig. 5a). Moreover, the CD spectra of the oligomers formed by the variant proteins were comparable to that of the WT protein oligomer. DLS spectra of the oligomers confirmed the presence of an oligomeric species of R_h ~16 nm, similar to that of WT protein oligomer (Fig. 5c).

Fluorescence spectra of the unlabelled W144−C153 and W197−C223 moPrP oligomers were also recorded (Fig. 5d). The emission maximum of the W197−C223 moPrP oligomer remained unchanged at 345 nm, but the fluorescence intensity was quenched compared to that of the monomer. On the other hand, for the W144−C153 moPrP oligomer, the emission maximum was blue shifted to 345 nm, with a concomitant increase in quantum yield, compared to that of the monomer.

4. Conclusion

The efficient oxidative refolding of single Trp, single Cys-containing mutant variant(s) of moPrP, containing a native disulfide bond, is demonstrated. The correct disulfide bond was formed at 1 M GdnHCl concentration, in the presence of reduced and oxidized glutathione in a 5:1 ratio. The proteins were purified as a
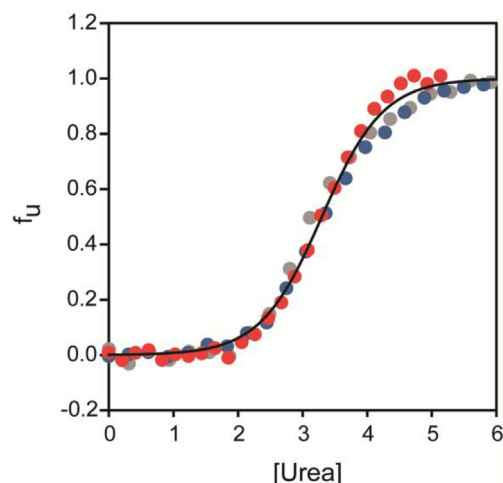
Fig. 6. Thermodynamic stabilities of mutant protein variants. Urea-induced equilibrium unfolding transitions of Trp-less (grey circles), W144—C153 (red circles) and W197—C223 (blue circles) moPrP at pH 4, 25 °C, as monitored by far-UV CD at 222 nm. The solid black line is a global fit of the denaturation profiles of all three proteins. (For interpretation of the references to colour in this figure legend, the reader is referred to the web version of this article.)

Table 1

Thermodynamic parameters obtained from urea-induced equilibrium unfolding studies of different moPrP variants at pH 4.

	ΔG (kcal mol^{-1})	C_m (M)
WT moPrP[a]	4.5	3.4
Trp-less moPrP	4.4	3.4
W144—C153C moPrP	4.3	3.3
W197-A223C moPrP	4.4	3.4

The m-value was constrained to 1.3 kcal mol^{-1} M^{-1} for all the moPrP variants.

[a] [29].

glutathione adduct of the additional cysteine, which was cleaved off before further experiments. The average yields of most mutant variants were found to be ~20 mg/L (~1 mg/g of wet cell weight). In addition, the protocol has been shown to be equally efficient for a protein which retains the native disulfide bond, but does not have an additional cysteine.

Unlabelled W144—C153 and W197—C223 moPrP as well as Trp-less moPrP, have been characterized thoroughly. The protocol has been implemented successfully for three other single Trp, single Cys-containing mutant variants of moPrP (data not shown), rendering it a good general purification strategy for purification of these proteins. Double cysteine-containing mutant variants for sm-FRET (single-molecule FRET) measurements have also been purified successfully using this protocol (data not shown). This provides an opportunity for making samples for many high-resolution spectroscopic measurements, especially those requiring large amounts of labelled protein, in a cost effective manner.

Acknowledgements

References

[1] L. Stryer, Fluorescence energy transfer as a spectroscopic ruler, Annu. Rev. Biochem. 47 (1978) 819—846.

[2] W.L. Hubbell, D.S. Cafiso, C. Altenbach, Identifying conformational changes with site-directed spin labeling, Nat. Struct. Biol. 7 (2000) 735—739.

[3] J.R. Gillespie, D. Shortle, Characterization of long-range structure in the denatured state of Staphylococcal Nuclease. I. Paramagnetic relaxation enhancement by nitroxide spin labels, J. Mol. Biol. 268 (1997) 158—169.

[4] L. Zhang, C.P. Chou, M. Moo-young, Disulfide bond formation and its impact on the biological activity and stability of recombinant therapeutic proteins produced by *Escherichia coli* expression system, Biotechnol. Adv. 29 (2011) 923—929, http://dx.doi.org/10.1016/j.biotechadv.2011.07.013.

[5] M. Berkmen, Production of disulfide-bonded proteins in *Escherichia coli*, Protein Expr. Purif. 82 (2012) 240—251, http://dx.doi.org/10.1016/j.pep.2011.10.009.

[6] M. Yang, C. Dutta, A. Tiwari, Disulfide-bond scrambling promotes amorphous aggregates in lysozyme and bovine serum albumin, J. Phys. Chem. B 119 (2015) 3969—3981, http://dx.doi.org/10.1021/acs.jpcb.5b00144.

[7] R. Rudolph, H. Lilie, In vitro folding of inclusion body proteins, FASEB J. 10 (1996) 49—56.

[8] R.R. Burgess, Refolding solubilized inclusion body proteins, Methods Enzymol. 463 (2009) 259—282, http://dx.doi.org/10.1016/S0076-6879(09)63017-2.

[9] B. Fisher, I. Sumner, P. Goodenough, Isolation, renaturation, and formation of disulfide bonds of eukaryotic proteins expressed in *Escherichia coli* as inclusion bodies, Biotechnol. Adv. 41 (1992) 3—13.

[10] C. Vendrely, H. Valadié, L. Bednarova, L. Cardin, M. Pasdeloup, J. Cappadoro, J. Bednar, M. Rinaudo, M. Jamin, Assembly of the full-length recombinant mouse prion protein I. Formation of soluble oligomers, Biochim. Biophys. Acta 1724 (2005) 355—366, http://dx.doi.org/10.1016/j.bbagen.2005.05.017.

[11] S. Jain, J.B. Udgaonkar, Evidence for stepwise formation of amyloid fibrils by the mouse prion protein, J. Mol. Biol. 382 (2008) 1228—1241, http://dx.doi.org/10.1016/j.jmb.2008.07.052.

[12] R. Zahn, C. Von Schroetter, K. Wu, Human prion proteins expressed in *Escherichia coli* and purified by high-affinity column refolding, FEBS Lett. 417 (1997) 400—404.

[13] Y. Arii, S. Oshiro, K. Wada, S. Fukuoka, Production of a recombinant full-length prion protein in a soluble form without refolding or detergents, Biosci. Biotechnol. Biochem. 75 (2011) 1181—1183, http://dx.doi.org/10.1271/bbb.100839.

[14] R.N.N. Abskharon, S. Ramboarina, H. El Hassan, W. Gad, M.I. Apostol, G. Giachin, G. Legname, J. Steyaert, J. Messens, S.H. Soror, A. Wohlkonig, A novel expression system for production of soluble prion proteins in *E.coli*, Microb. Cell Fact. 11 (2012) 1—11.

[15] N.K. Chu, C.F.W. Becker, Recombinant expression of soluble murine prion protein for C-terminal modification, FEBS Lett. 587 (2013) 430—435, http://dx.doi.org/10.1016/j.febslet.2012.12.026.

[16] M.P. McKinley, D.C. Bolton, S.B. Prusiner, A protease-resistant protein is a structural component of the Scrapie prion, Cell 35 (1983) 57—62, http://dx.doi.org/10.1016/0092-8674(83)90207-6.

[17] O. Inanami, S. Hashida, D. Iizuka, M. Horiuchi, W. Hiraoka, Y. Shimoyama, H. Nakamura, F. Inagaki, M. Kuwabara, Conformational change in full-length mouse prion: a site-directed spin-labeling study, Biochem. Biophys. Res. Commun. 335 (2005) 785—792, http://dx.doi.org/10.1016/j.bbrc.2005.07.148.

[18] Y. Sun, L. Breydo, N. Makarava, Q. Yang, O.V. Bocharova, I.V. Baskakov, Site-specific conformational studies of prion protein (PrP) amyloid fibrils revealed two cooperative folding domains within amyloid structure, J. Biol. Chem. 282 (2007) 9090—9097, http://dx.doi.org/10.1074/jbc.M608623200.

[19] B.Y. Lu, J.Y. Chang, A 3-disulfide mutant of mouse prion protein expression, oxidative folding, reductive unfolding, conformational stability, aggregation and isomerization, Arch. Biochem. Biophys. 460 (2007) 75—84, http://dx.doi.org/10.1016/j.abb.2006.12.014.

[20] V. Dalal, S. Arya, M. Bhattacharya, S. Mukhopadhyay, Conformational switching and nanoscale assembly of human prion protein into polymorphic amyloids via structurally labile oligomers, Biochemistry 54 (2015) 7505—7513, http://dx.doi.org/10.1021/acs.biochem.5b01110.

[21] C. Yang, W.L. Lo, Y.H. Kuo, J.C. Sang, C.Y. Lee, Y.W. Chiang, R.P.Y. Chen, Revealing structural changes of prion protein during conversion from alpha-helical monomer to beta-oligomers by means of ESR and nanochannel encapsulation, ACS Chem. Biol. 10 (2015) 493—501, http://dx.doi.org/10.1021/cb500765e.

[22] A.C. Apetri, W.K. Surewicz, Kinetic intermediate in the folding of human prion protein, J. Biol. Chem. 277 (2002) 44589—44592, http://dx.doi.org/10.1074/jbc.C200507200.

[23] A.C. Apetri, K. Maki, H. Roder, W.K. Surewicz, Early Intermediate in human prion protein folding as evidenced by ultrarapid mixing experiments, J. Am. Chem. Soc. 128 (2006) 11673—11678.

[24] T. Hart, L.L.P. Hosszu, C.R. Trevitt, G.S. Jackson, J.P. Waltho, J. Collinge, A.R. Clarke, Folding kinetics of the human prion protein probed by temperature jump, Proc. Natl. Acad. Sci. U. S. A. 106 (2009) 5651—5656, http://dx.doi.org/10.1073/pnas.0811457106.

[25] R.P. Honda, M. Xu, K.I. Yamaguchi, H. Roder, K. Kuwata, A native-like intermediate serves as a branching point between the folding and aggregation pathways of the mouse prion protein, Structure 23 (2015) 1735—1742, http://

dx.doi.org/10.1016/j.str.2015.07.001.

[26] W. Swietnicki, M. Morillas, S.G. Chen, P. Gambetti, W.K. Surewicz, Aggregation and fibrillization of the recombinant human prion protein huPrP90-231, Biochemistry 39 (2000) 424–431, http://dx.doi.org/10.1021/bi991967m.

[27] F. Eghiaian, T. Daubenfeld, Y. Quenet, M. Van Audenhaege, A. Bouin, G. Van der Rest, J. Grosclaude, H. Rezaei, Diversity in prion protein oligomerization pathways results from domain expansion as revealed by hydrogen/deuterium exchange and disulfide linkage, Proc. Natl. Acad. Sci. U. S. A. 104 (2007) 7414–7419, http://dx.doi.org/10.1073/pnas.0607745104.

[28] N.J. Cobb, F.D. Sönnichsen, H. McHaourab, W.K. Surewicz, Molecular archi-tecture of human prion protein amyloid: a parallel, in-register beta-structure, Proc. Natl. Acad. Sci. U. S. A. 104 (2007) 18946–18951, http://dx.doi.org/10.1073/pnas.0706522104.

[29] J. Singh, J.B. Udgaonkar, Molecular mechanism of the misfolding and oligo-merization of the prion protein: current understanding and its Implications, Biochemistry 54 (2015) 4431–4442, http://dx.doi.org/10.1021/acs.biochem.5b00605.

[30] W. Swietnicki, R.B. Petersen, P. Gambetti, W.K. Surewicz, Familial mutations and the thermodynamic stability of the recombinant human prion protein, J. Biol. Chem. 273 (1998) 31048–31052, http://dx.doi.org/10.1074/jbc.273.47.31048.

[31] K. Kuwata, N. Nishida, T. Matsumoto, Y.O. Kamatari, J. Hosokawa-Muto, K. Kodama, H.K. Nakamura, K. Kimura, M. Kawasaki, Y. Takakura, S. Shirabe, J. Takata, Y. Kataoka, S. Katamine, Hot spots in prion protein for pathogenic conversion, Proc. Natl. Acad. Sci. U. S. A. 104 (2007) 11921–11926, http://dx.doi.org/10.1073/pnas.0702671104.

[32] S.H. Bae, G. Legname, A. Serban, S.B. Prusiner, P.E. Wright, H.J. Dyson, Prion proteins with pathogenic and protective mutations show similar structure and dynamics, Biochemistry 48 (2009) 8120–8128, http://dx.doi.org/10.1021/bi900923b.

[33] R. Riek, S. Hornemann, G. Wider, M. Billeter, R. Glockshuber, K. Wüthrich, NMR structure of the mouse prion protein domain PrP(121-231), Nature 382 (1996) 180–182, http://dx.doi.org/10.1038/382180a0.

[34] G.S. Jackson, L.L.P. Hosszu, A. Power, A.F. Hill, J. Kenney, H. Saibil, C.J. Craven, J.P. Waltho, A.R. Clarke, J. Collinge, Reversible conversion of monomeric hu-man prion protein between native and fibrilogenic conformations, Science 283 (1999) 1935–1937, http://dx.doi.org/10.1126/science.283.5409.1935.

[35] N.R. Maiti, W.K. Surewicz, The role of disulfide bridge in the folding and stability of the recombinant human prion protein, J. Biol. Chem. 276 (2001) 2427–2431, http://dx.doi.org/10.1074/jbc.M007862200.

[36] Y. Watanabe, O. Inanami, M. Horiuchi, W. Hiraoka, Y. Shimoyama, F. Inagaki, M. Kuwabara, Identification of pH-sensitive regions in the mouse prion by the cysteine-scanning spin-labeling ESR technique, Biochem. Biophys. Res. Com-mun. 350 (2006) 549–556, http://dx.doi.org/10.1016/j.bbrc.2006.09.082.

[37] S. Hornemann, C. Korth, B. Oesch, R. Riek, G. Wider, K. Wuthrich, R. Glockshuber, Recombinant full-length murine prion protein, mPrP(23-231): purification and spectroscopic characterization, FEBS Lett. 413 (1997) 277–281, http://dx.doi.org/10.1016/S0014-5793(97)00921-6.

[38] J. Hosokawa-muto, K. Yamaguchi, Y.O. Kamatari, Synthesis of double-fluorescent labeled prion protein for FRET analysis, Biosci. Biotechnol. Bio-chem. 79 (2015) 37–41, http://dx.doi.org/10.1080/09168451.2015.1050991.

[39] R. Moulick, R. Das, J.B. Udgaonkar, Partially unfolded forms of the prion pro-tein populated under misfolding-promoting conditions, J. Biol. Chem. 290 (2015) 25227–25240, http://dx.doi.org/10.1074/jbc.M115.677575.

[40] D.C. Jenkins, D.S. Pearson, A. Harvey, I.D. Sylvester, M.A. Geeves, T.J.T. Pinheiro, Rapid folding of the prion protein captured by pressure-jump, Eur. Biophys. J. 38 (2009) 625–635, http://dx.doi.org/10.1007/s00249-009-0420-6.

[41] V.R. Agashe, J.B. Udgaonkar, Thermodynamics of denaturation of Barstar: evidence for cold denaturation and evaluation of the interaction with gua-nidine hydrochloride, Biochemistry 34 (1995) 3286–3299.